Analyst

Simple Distance-based Thread Analytical Device Integrated with Ion Imprinted Polymer for Zn2+ Quantification in Human Urine Samples

Journal:	*Analyst*
Manuscript ID	AN-ART-01-2024-000076.R1
Article Type:	Paper
Date Submitted by the Author:	29-Feb-2024
Complete List of Authors:	Chheang, Lita; Tufts University, Department of Electrical and Computer Engineering Khachornsakkul, Kawin; Tufts University, Electrical and Computer Engineering Del-Rio-Ruiz, Ruben; Tufts University, Electrical and Computer Engineering Zeng, Wenxin; Tufts University, Department of Electrical and Computer Engineering; Tufts University, Nanolab Thongkon, Nisakorn ; King Mongkut's University of Technology Thonburi, Chemistry Thanasupsine, Sudtida; King Mongkut's University of Technology Thonburi, Chemistry Sonkusale, Sameer; Tufts University, Department of Electrical and Computer Engineering

Simple Distance-based Thread Analytical Device Integrated with Ion Imprinted Polymer for Zn^{2+} Quantification in Human Urine Samples

Lita Chheang,[a,b,c,d*] Kawin Khachornsakkul,[a,b*] Ruben Del-Rio-Ruiz,[a,b] Wenxin Zeng,[a,b] Nisakorn Thongkon,[c] Sudtida Pliankarom Thanasupsin,[e] Sameer Sonkusale,[a,b*]

[a]Department of Electrical and Computer Engineering, Tufts University, Medford, MA 02155, USA

[b]Nano Lab, Tufts University, Medford, MA 02155, USA

[c]Department of Chemistry, Faculty of Science, King Mongkut's University of Technology Thonburi, Bangkok 10140, Thailand

[d]Department of Chemistry, Faculty of Science, Royal University of Phnom Penh, Federation of Russia Blvd, Tuol Kork, Phnom Penh, Cambodia

[e]Chemistry for Green Society and Healthy Living Research Unit, Faculty of Science, King Mongkut's University of Technology Thonburi, Bangkok 10140, Thailand

*To whom correspondence should be addressed. Email: lita.chheang@tufts.edu Kawin.khachornsakkul@tufts.edu sameer.sonkusale@tufts.edu

Abstract

This article presents the development of a distance-based thread analytical device (dTAD) integrated with ion-imprinted polymer (IIP) for quantitative monitoring of zinc ions (Zn^{2+}) in human urine samples. The IIPs was chemically and easily modified on the thread channel using dithizone (DTZ) as a ligand to bind to Zn^{2+} with methacrylic acid (MAA) as a functional monomer and ethylene glycol dimethacrylate (EGDMA) as well as 2,2-azobisisobutyronitrile (AIBN) as cross-linking agents to enhance the selectivity for Zn^{2+} detection. The imprinted polymer was characterized using Attenuated Total Reflectance-Fourier Transform Infrared (ATR-FTIR) spectroscopy and Scanning Electron Microscopy-Energy Dispersive X-ray Spectroscopy (SEM-

EDS). Under optimization, the linear detection range was obtained from 1.0 to 20.0 mg L^{-1} (R^2 = 0.9992) with the limit of (LOD) of 1.0 mg L^{-1}. Other interfering metal ions and molecules did not interfere with this approach, leading to high selectivity. Furthermore, our technique exhibits a remarkable recovery ranging from 100.48 % to 103.16 %, with the highest relative standard deviation (%RSD) of 5.44 % for monitoring Zn^{2+} in human control urine samples, indicating high accuracy and precision. Similarly, there is no significant statistical difference between the results obtained using our method compared to standards on zinc supplement sample labels. The proposed method offers several advantages in detecting trace Zn^{2+} for point-of-care (POC) medical diagnostics and environmental sample analysis, such as ease of use, instrument-free readout, and cost efficiency. Overall, our developed dTADs-based IIPs method holds potential for simple, affordable, and rapid detection of Zn^{2+} level and can be applied to other metal ions analysis.

Keywords: Distance-based thread analytical devices (dTADs), ion-imprinted polymers (IIPs), point of care diagnostics (POC), urine sample, Zn^{2+}detection.

1. Introduction

Zinc (Zn^{2+}) is an essential nutrient for the human body since it can trigger and assist the immune system in reducing inflammatory responses. [1–6] This metal ion plays an important role in neurotransmission, cell division, catalytic functions, and protein synthesis. The normal concentration of Zn^{2+} in human individuals is approximately 0.33 mg/kg/day. [3,7] However, its higher concentration can cause periorificial dermatitis, alopecia, nausea, diarrhea, and headaches. [2,8–11] Conversely, Zn^{2+} deficiency can reduce immune function and lead to neurological disorders. In general, the concentration of Zn^{2+} is 1.19 mg L^{-1} for males and 1.16 mg L^{-1} for females; [12–14] with elevated levels resulting in aforementioned disorders. [8,11,15] It is more convenient to determine Zn^{2+} levels regularly by analyzing urine samples rather than using blood samples which involves invasive sample collection procedure and may result in infection.

Several effective methods have been developed for Zn^{2+} determination, including atomic absorption spectroscopy, [16] gamma spectrometry, [17] immunochromatographic assay, [18] inductively coupled plasma mass spectrometry (ICP-MS), [19] inductively coupled plasma optical emission spectroscopy (ICP-OES), [20] atomic fluorescence spectrometry, [21] stripping voltammetry, [22–24] differential pulse voltammetry, [25] potentiometric methods, [22,26,27] chronopotentiometry analysis, [28] light scattering, [29] laser-induced breakdown spectroscopy, [30] laser desorption/ionization mass spectrometry, (LDI-MS) [31] and chromatographic techniques (HPLC). [32] Even though these methods provide high sensitivity and selectivity for Zn^{2+} monitoring, they are also limited for point of care (POC) testing owing to their large size and higher cost of analysis and time. Developing a portable and affordable analytical tool for on-site detection is needed.

Recently, microfluidic thread-based analytical devices (μTADs) have gained more attention due to their simplicity, cost-effectiveness, rapid response, and ease of operation. [33–37] Since they allow the fluid to flow on the hydrophilic channel by capillary force, there is no need for an external microfluidic pump, saving cost and reducing overall complexity. Of all the readout methods for point of testing, distance-based visual measurement offers a simpler approach without the need for instrumentation. The signal output is a colored distance signal, which can be easily read by tools like cameras and smartphones. Compare this to other forms of signal readout, such as measuring intensity of the colorimetric output or the spectroscopic change in color, both of which are sensitive to background lighting, and harder to quantify without dedicated hardware. The rationale for using threads over paper as a substrate stems from their inherent advantages [38–40] such as a natural self-contained microfluidic channel which does not need any patterning with a hydrophobic material like wax. Moreover, it is easy to pre-deposit reagents and chemicals on threads through simple dip coating. Typically, upon introducing a solution containing analyte on the thread, it flows along the thread as open capillary channel and reacts with a pre-deposited reagent, causing color change along the length of the thread upon interaction with the target. The analyte concentration can be

determined by measuring this colored distance on the thread with a traditional ruler without the need for any instrumentation. Previously, our group had developed dTADs for melatonin monitoring relying on the reaction between melatonin and 2,3-naphthalenedialdehyde (2,3-Nda), which caused the color to change from colorless to yellow, with distance length directly proportional to the melatonin level. [41] Furthermore, Singhaphan et al. [42] presented a dTAD sensor for nitrite ion (NO_2^-) detection using the Griess reaction. The color distance length changed from colorless to pink with increased NO_2^- concentration. These examples show that the dTAD sensor can be a simple and effective alternative tool for POC and on-site monitoring.

To enhance assay selectivity for metal ion detection, ion-imprinted polymers (IIPs) techniques have been widely deployed for its high affinity to target ions and reduced cost and time of synthesis. [43–47] Generally, IIPs are synthetic polymers that recognize the target imprinted ion and are used primarily to separate the target ion from other ions and/or molecules in a matrix. [43,44,46,48–54] For example, Shamsipur et al. [43] presented the ion-imprinted polymeric nanoparticles for selective separation and sensitive determination of zinc ions in different matrices. Herein report the integration of IIPs with dTAD sensors for the first time.

In this study, we successfully developed a simple and low-cost dTAD sensor integrated with IIPs for Zn^{2+} determination in human urine samples. Dithizone (DTZ) is used as a chromogenic substrate for the colorimetric detection of Zn^{2+}. The dTADs is simply prepared by depositing chromogenic substrate, monomer, cross-linker, and initiator onto the cotton thread. A color change between green and pink is observed when the template is removed during the formation of IIP. Quantitative detection of Zn^{2+} is simply conducted by measuring the distance length of the pink color. The sensor is selective to Zn^{2+} at clinically relevant levels in human urine samples with desirable cost-effectiveness, portability, ease of operation, and user-friendliness. Likewise, to the best of our knowledge, this is the first demonstration of a dTAD sensor for Zn^{2+} measurement

relying on the use of IIPs. This platform can also be extended towards the detection of other metal ions in complex biological media.

2. Experimental

2.1 Chemicals and materials

Zinc chloride ($ZnCl_2$), dithizone (DTZ), methacrylic acid (MAA), ethylene glycol dimethacrylate (EGDMA), azobisisobutyronitrile (AIBN), hydrochloric acid (HCl), sodium bicarbonate (Na_2CO_3), bovine serum albumin (BSA), creatinine, fructose, glucose, lactic acid, and uric acid were purchased from Sigma-Aldrich Inc., USA. Urea was obtained from Tokyo Chemical Industry Co. Ltd (Japan). All chemicals used in the experiment were analytical reagents (AR grade). Cotton thread was purchased from Michael's store (MA, USA); it was made up of 3 separate strands with each strand of diameter 1.201 mm, and 15 twists per inch measured using microscopy Fig. S1. Vortex mixer was obtained from Fisher Scientific. The fabrication of the supporting platform is described in Fig. S2 and Fig. S3.

2.2. Instrumentation

The morphological investigation of this developed techniques was studied using the FTIR spectra (Thermo Fisher Scientific Nicolet 6700, USA) and Scanning Electron Microscope (SEM; Axia ChemiSEM, ThermoFisher Scientific, USA). The color intensity detection of the developed thread was performed using ColorGrab application on smartphone (OPPO A54) under an LED lamp (Racer Katie ECO LED Daylight A60, 6500K, 3W, China), as indicated Fig. S4. [55,56]

2.3. Fabrication of the IIPs-based dTADs for detection of Zn^{2+} ions

Firstly, the IIP solution for Zn^{2+} (Zn-IIPs) was prepared by mixing 1.0 mL of Zn^{2+} (40.0 mg L^{-1}) and DTZ (0.20 mmol L^{-1}), 25.0 µL of MAA, 30.0 µL of EGDMA, and 20.0 µL of AIBN. Afterwards, the mixed solution was vortexed for 1 min. To modify the thread, the threads were cut

to 14.0 cm in length and socked in 50.0 mL of Na_2CO_3 solution (1.0 mol L^{-1}) for 2 hrs. to remove their natural wax on the surface. Next, it is washed until its pH is natural and then dried in the oven at 105 ºC for 10 min. Subsequently, these prepared threads were fixed into the supporting platform by assisting with scotch tape. Next, 200.0 µL of Zn-IIPs is deposited on the thread and let dry at room temperature by avoiding the light, as indicated in Fig. 1a. The Zn^{2+} template is removed from the thread channel by dropping hydrochloric acid (HCl) at 0.50 mol L^{-1}, and the prepared dTAD sensors were kept in the dark place. No-IIP based dTADs were also prepared by immobilizing DTZ into the thread channel without any ion imprinting.

2.4. General optimization of IIPs-based dTADs for Zn (II) detection

To optimize sample volume and reaction time, we measured the distance signals of Zn^{2+} concentration at 20.0 mg L^{-1} (Fig. 1b). Furthermore, the concentration of template, ligand, and extraction solvent, volume of monomer, cross-linker, and initator, and vortex time were evaluated by measuring the color intensity on the thread using Red-Green-Blue (RGB) mode of Image J. All experiment was conducted for three times reproducibility (n=3).

2.5. Analytical procedure

100.0 µL of Zn^{2+} solutions at various concentrations introduced into the IIPs-based dTADs sensor. After 10 min, the distance signal of pink color in the thread was measured. The linear range was plotted between Zn^{2+} concentration and its distance signals. The detection limit (LOD) was evaluated by naked-eye readout at the lowest Zn^{2+} concentration, obtaining the initial pink color on the dTAD sensor. The selectivity and interference were further studied via the measurement of the distance signal of Zn^{2+} at 2.0 mg L^{-1}, compared with other interferents expected to be in real samples. All experiments in the developed method were reproduced in triplicates (n=3). Images were taken with the smartphone's camera (iPhone 8+).

2.6. Real sample analysis

1.0 mL of human control urine samples containing Zn^{2+} at different concentrations were dropped into the developed dTAD sensor and followed the analytical procedure. The recovery percentage was then calculated by detecting Zn^{2+} in the developed method. Likewise, 20 tablets of zinc supplement samples were crushed and weighed precisely, subsequently dissolved in DI water. Afterwards, 1.0 mL of supplement sample solutions were introduced into the developed dTAD sensor and continued following the analytical procedure. The resultant Zn^{2+} concentrations were calculated and statistically compared with their labels.

3. Results and Discussion

3.1 Characterization of IIPs-based dTADs for Zn^{2+} detection

The morphology of dTAD was characterized by SEM images, as shown in Fig. S5. The outermost layer of natural cotton fibers is typically covered in wax. [57–59] Most of the wax is composed of long fatty acid chains, which renders cotton fibers hydrophobic and diminishes the material's capacity to wick liquid. To remove the wax and enhance the hydrophilic property of the thread, we treated the thread with Na_2CO_3 solution, resulting in a higher amount of the hydroxyl (–OH) groups on the surface of the thread. [60,61] After imprinting polymer, we noticed that the surface of the thread is rougher with zinc content (Fig. S5(c)). The surface of the thread was smoother after template removal (Fig. S5(d)). With the above results, we show successful imprinting of the IIP onto the thread substrate for selective determination of Zn^{2+} concentration. Furthermore, we characterized the structure of the developed dTAD sensor using FTIR spectra, as shown and described in Fig. S6.

3.2 Optimization of IIPs-based dTADs for Zn (II) detection

To test whether the IIPs-based dTADs can enhance the assay performance for Zn^{2+} detection, we measured the distance length of the pink color onto the thread channel when solution containing Zn^{2+} at 5.0 mg L^{-1} was introduced into the sample zone of the device. In Fig. 2, we observed that

the distance signal of the blank was 0.0 cm (Fig. 2(a)), while it increased to 1.37 cm when the Zn^{2+} solution was introduced (Fig. 2(c)). Notably, there was no distance signal measured on the dTAD with no-IIP similar to the blank signal (Fig. 2(b)). In the latter case, the pale pink color of DTZ and Zn^{2+} on the thread channel was unstable and rapidly disappeared, making it impossible to measure the distance signal. Whereas, the utilization of IIP integrated with the dTAD enabled the stable measurement of Zn^{2+} by complexing with the DTZ reagent.

In our experiment, the Zn^{2+} template and DTZ concentrations were optimized by detecting the pink color intensity. We observed that the highest intensity was found when Zn^{2+} template and DTZ were 40.0 mg $L^{-1}$and 0.20 mmol L^{-1}, respectively (Fig. S7 (a and b)). The utilization of higher DTZ concentration leads to a lower pink intensity on the thread. Similarly, the larger template concentration results in difficult template removal, affecting the signal measurement. In addition, the volume of monomer and cross-linker was studied, as it can affect the formation of imprinting polymer. We noticed that the intensity of the pink color increased with their concentration and stabilized when their volumes were 25.0, 30.0, and 20.0 for MAA, EGDMA, and AIBN, respectively, (Fig. S7 (c-e)). Possibly, at higher volumes, the number of binding cavities on the thread substrate had saturated. Therefore, we selected these volumes as sufficient monomer and cross-linker levels for our work. Moreover, HCL concentration was investigated since it affects the template removal. The result demonstrated that there was an increase in the color intensity as its concentration increased until 0.50 mol L^{-1}, and beyond that level, the intensity reduced (Fig. S7(f)). This is due to the fact that having too much acid disrupts the structure of IIPs in the thread substrate. Thus, the concentration of HCL at 0.50 mol L^{-1} was chosen in this proposed method.

Moreover, we investigated the sample volume of Zn^{2+} solution between 70.0 and 120.0 µL. The result indicated an increase in the distance lengths as the sample volume increased. However, the distance signals gradually reduced after the sample volume exceeded 100.0 µL. This is because the sample leaks from the thread at higher volumes, leading to reduced Zn^{2+} content. So, we chose

the sample volume of 100.0 μL as an optimum level in our proposed method Fig. S8(c). We also studied the reaction time by counting the time after the introduction of the sample solution onto the thread. We observed an increase in the distance signal reaching a constant length when the time was over 10.0 min (Fig. S8(d)). Therefore, 10 min was selected as an adequate reaction time for our experiment, which is quite low for portable on-site analysis.

3.3 Analytical characteristics

The analytical performance of the proposed IIPs-based dTADs sensor for quantitative Zn^{2+} detection was further studied under optimal conditions. According to Fig. 3, the average distance signal of the pink color for detecting Zn^{2+} at 1.0 mg L^{-1} was 0.45 cm (Fig. 3(b)). This value was distinguishable from the signal obtained from the blank sample (Fig. 3(a)). Subsequently, it can be observed that there is a direct correlation between the concentration of Zn^{2+} and the average distance of signals, as depicted in Fig. 3(b-f). Furthermore, the linear range of our developed dTADs from 1.0 to 20.0 mg L^{-1} (R^2 = 0.9992) was obtained, as shown in Fig. 3(g). The LOD was determined by measuring the lowest distance length for Zn^{2+} detection by naked-eye observation. We found that the shortest distance signal of 0.45 ± 0.05 cm was acquired when detecting Zn^{2+} at 1.0 mg L^{-1} (Fig. S9). Similarly, we measured this concentration ten times (n = 10) to calculate the measurement uncertainty for our assay validation.[62] The result indicated that the average distance signal of this level was 0.46 cm. So, we could confirm that the LOD of the proposed method for Zn^{2+} detection is 1.0 mg L^{-1}.

3.4 Selectivity and interferent studies

The selectivity of the proposed technique was evaluated through the detection of the distance signal Zn^{2+} at 2.0 mg L^{-1} compared to the signal obtained from other substrates. These potential interferences included glucose (10.0 mmol L^{-1}), bovine serum albumin (10.0 g L^{-1}), lactic acid

(50.0 μmol L^{-1}), uric acid (500.0 μmol L^{-1}), urea (50.0 mmol L^{-1}), and creatinine (1.0 g L^{-1}). Fig. 4(a) showed that only Zn^{2+} exhibited a distinct distance signal from zero, whereas the signals from other substrates remained comparable to the blank signals. Likewise, we measured the distance signal of the mixture solution between Zn^{2+} at 2.0 mg L^{-1} and other interferences. In Fig. 4(b), the results indicated that there were no significant differences in distance signals between measuring only Zn^{2+} solution and the mixture solution. As a result, it can be inferred that our assay is selective to the Zn^{2+}.

3.5 Application in real samples

To validate the applicability of the proposed method, we spiked different concentrations of Zn^{2+} at 3.0, 5.0, and 7.0 mg L^{-1} into the human control urine, and the spiked solutions were introduced into the developed dTADs. We determined the sample distance signal for these levels and then interpreted it to Zn^{2+} concentration using the standard linear range presented in Fig. 3(g). In Table 1, the recovery percentage ranges from 100.48% to 103.16%, with the highest relative standard deviation (RSD) of 5.44%. Likewise, we used our device to determine the Zn^{2+} concentration in a commercial Zinc supplement product sample and compared to its concentration labelled on the product. In Table 2, we noticed no dramatical differences in concentration between our method and the value reported on the product label at 95% confidence level of t-test statistics ($T_{critical}$ = 4.30). Therefore, our method could detect Zn^{2+} concentration with acceptable accuracy and precision.

3.6 Comparison of our proposed method and other methods

Table 3 demonstrates a comparison of the analytical performance of our developed dTADs method with other electrochemical, colorimetric, and optical methods for monitoring Zn^{2+} concentration.[41,48-50] While the previous techniques exhibited higher sensitivity with a lower LOD than our technique, they required expensive instruments such as potentiostats and optical analyzers for signal readout, increasing analysis costs which may limit its accessibility for unskilled users.

Importantly, our dTADs can monitor Zn^{2+} levels in human urine samples within the generally accepted clinical range.[12-14] To conclude, our proposed technique for Zn^{2+} determination is more affordable and simpler than previous methods in terms of signal readout and practicality.

4. Conclusion

Herein, we successfully developed the IIPs-based dTAD sensor for determining Zn^{2+} levels in human urine samples. This study is the first demonstration of an integrated thread-based analytical device with IIPs for metal ions analysis in a complex biological matrix. Use of IIP was shown to enhance the selectivity of the assay and distance-based measurement was shown to facilitate simpler quantitative readout. The distance-based measurement of Zn^{2+} concentration was easily monitored by measuring the extent of pink color length due to the stable interaction of DTZ with Zn^{2+} in presence of IIP on the thread without the need for any instrument. Due to the nature of IIP, this technique exhibits high selectivity with no interference from other metal ions that may also cause color change on its reaction with the DTZ substrate. Moreover, the total analysis time is just 10 min after sample introduction, indicating rapid analysis time for on-site application. Likewise, our assay showed high accuracy and precision by detecting Zn^{2+} concentration in human control urine samples and for monitoring quality of Zinc supplements. Overall, our developed method has many advantages, including simplicity, rapid response, cost-effectiveness, and ease of operation. This method can also be extended to selectively determine other metal ions in complex biological media. This will facilitate timely prognosis and diagnosis of different diseases that involve metal ions in disease pathways.

Credit author statement

Lita Chheang: Conceptualization, Methodology, Investigation, Validation, Data curation, Visualization, Writing - original draft. Kawin Khachornsakkul: Method Validation, Supervision, Writing – original draft, review and editing. Ruben Del-Rio-Ruiz: Base platform fabrication, Writing – review and edit. Wenxin Zeng: SEM-EDS. Nisakorn Thongkon: Method Validation.

Sudtida Pliankarom Thanasupsin: Supervision. Sameer Sonkusale: Resources, Project administration, Supervision, Writing - review and editing.

Conflicts of interest

There are no conflicts to declare.

Acknowledgements

This study was financially supported by the Nano Lab and Department of Electrical and Computer Engineering, Tufts University, Medford, MA 02155, USA. Dr. Chheang was supported by the Petchra Pra Jom Klao Ph.D. Research Scholarship, Thailand. The time and effort of other personnel from Tufts University were supported by the National Science Foundation (NSF) under Grant 1931978, the TTW program at the Uniformed Services University of Health Sciences (USUHS) under award HU0001-20-2-0014, and the DoD Peer Review Medical Research Program under award number W81XWH-21-2-0012. We are also grateful for the support from Nano Lab team members for their insightful information and versatile assistance during the experiments.

References

1 D. P. Kiouri, E. Tsoupra, M. Peana, S. P. Perlepes, M. E. Stefanidou and C. T. Chasapis, *EXCLI Journal*, 2023, **22**, 809–827.

2 L. M. Plum, L. Rink and H. Hajo, *International Journal of Environmental Research and Public Health*, 2010, **7**, 1342–1365.

3 K. Jomova, M. Makova, S. Y. Alomar, S. H. Alwasel, E. Nepovimova, K. Kuca, C. J. Rhodes and M. Valko, *Chemico-Biological Interactions*, 2022, **367**, 110173.

4 S. A. Read, S. Obeid, C. Ahlenstiel and G. Ahlenstiel, *Advances in Nutrition*, 2019, **10**, 696–710.

5 L. Chheang, N. Thongkon, T. Sriwiriyarat and S. P. Thanasupsin, *Sustainability (Switzerland)*, 2021, **13**, 1–20.

6 L. Chheang, P. Limsuwan, N. Thongkon, T. Sriwiriyarat and S. P. Thanasupsin, *Water (Switzerland)*, , DOI:10.3390/w15081566.

7 J. Luo, T. Zhu, M. Jin, X. Cheng, Y. Yuan, X. Wang, J. Lu, L. Jiao, D. R. Tocher and Q. Zhou, *British Journal of Nutrition*, 2020, **124**, 681–692.

8 C. Livingstone, *Nutrition in Clinical Practice*, 2015, **30**, 371–382.

9 N. Z. Gammoh and L. Rink, *Nutrients*, , DOI:10.3390/nu9060624.

10 C. T. Chasapis, P. S. A. Ntoupa, C. A. Spiliopoulou and M. E. Stefanidou, *Archives of Toxicology*, 2020, **94**, 1443–1460.

11 R. S. Gibson, *Plant and Soil*, 2012, **361**, 291–299.

12 H. H. SANDSTEAD and W. AU, in *Handbook on the Toxicology of Metals*, Elsevier, Inc., Third Edit., 2007, pp. 925–947.

13 G. F. Nordberg, B. A. Fowler and N. Monica., *Handbook on the Toxicology of Metals*, Elsevier, London, 4th edn., 2014.

14 F. P. Phiri, E. L. Ander, R. M. Lark, E. J. M. Joy, A. A. Kalimbira, P. S. Suchdev, J. Gondwe, E. M. Hamilton, M. J. Watts and M. R. Broadley, *Environmental Geochemistry and Health*, 2021, **43**, 259–271.

15 A. S. Prasad, *Discovery of Zinc for Human Health and Biomarkers of Zinc Deficiency*, Elsevier Inc., 2017.

16 H. Uslu, Ç. Büyükpınar, T. Unutkan, H. Serbest, N. SAN, F. Turak and S. Bakırdere, *Microchemical Journal*, 2018, **137**, 155–159.

17 Ž. Grahek, M. Rožmarić Mačefat and S. Lulić, *Analytica Chimica Acta*, 2006, **560**, 84–93.

18 Y. Tang, Y. F. Zhai, J. J. Xiang, H. Wang, B. Liu and C. W. Guo, *Environmental Pollution*, 2010, **158**, 2074–2077.

19 D. Larivière, K. M. Reiber, R. D. Evans and R. J. Cornett, *Analytica Chimica Acta*, 2005, **549**, 188–196.

20 L. Zhao, S. Zhong, K. Fang, Z. Qian and J. Chen, *Journal of Hazardous Materials*, 2012, **239–240**, 206–212.

21 Q. Zhou, N. Zhao and G. Xie, *Journal of Hazardous Materials*, 2011, **189**, 48–53.

22 V. B. Dos Santos, E. L. Fava, N. S. De Miranda Curi, R. C. Faria and O. Fatibello-Filho, *Talanta*, 2014, **126**, 82–90.

23 F. C. Vicentini, T. A. Silva, A. Pellatieri, B. C. Janegitz, O. Fatibello-Filho and R. C. Faria, *Microchemical Journal*, 2014, **116**, 191–196.

24 Z. Bi, P. Salaün and C. M. G. van den Berg, *Analytica Chimica Acta*, 2013, **769**, 56–64.

25 M. K. Bojdi, M. H. Mashhadizadeh, M. Behbahani, A. Farahani, S. S. H. Davarani and A. Bagheri, *Electrochimica Acta*, 2014, **136**, 59–65.

26 I. A. Oke, S. Lukman, A. Ismail, E. O. Fehintola and J. S. Amoko, *Removal of lead ions from water and wastewaters electrochemically*, Elsevier Inc., 2017.

27 J. Pizarro, R. Segura, D. Tapia, F. Navarro, F. Fuenzalida and M. Jesús Aguirre, *Food Chemistry*, 2020, **321**, 126682.

28 R. O. Kadara and I. E. Tothill, *Analytica Chimica Acta*, 2008, **623**, 76–81.

29 K. J. Tan, C. Z. Huang and Y. M. Huang, *Talanta*, 2006, **70**, 116–121.

30 S. T. Järvinen, J. Saarela and J. Toivonen, *Spectrochimica Acta - Part B Atomic Spectroscopy*, 2013, **86**, 55–59.

31 H. Y. Wu, B. Unnikrishnan and C. C. Huang, *Sensors and Actuators, B: Chemical*, 2014, **203**, 880–886.

32 Y. Y. Qiufen Hu, Guangyu Yang, Jiayuan Yin, *Journal of Analytical Chemistry*, 2002, **58**, 1054–1059.

33 K. Khachornsakkul, R. Del-Rio-Ruiz, L. Chheang and S. Sonkusale, *Sensors and Actuators B: Chemical*, 2023, **395**, 134518.

34 R. Shimazu, K. Tomimuro, Y. Ni, C. Malegori, V. Hamedpour, Y. Hiruta, P. Oliveri, M. Merkx and D. Citterio, *Sensors and Actuators B: Chemical*, 2022, **352**, 131002.

35 A. C. M. Oliveira, D. A. G. Araújo, L. A. Pradela-Filho, R. M. Takeuchi, M. A. G. Trindade and A.

L. dos Santos, *Lab Chip*, 2022, **22**, 3045–3054.

36 P. Erfle, J. Riewe, S. Cai, H. Bunjes and A. Dietzel, *Lab on a Chip*, 2022, **22**, 3025–3044.

37 X. Weng, Y. Kang, Q. Guo, B. Peng and H. Jiang, *Biosensors and Bioelectronics*, 2019, **132**, 171–185.

38 P. Mostafalu, M. Akbari, K. A. Alberti, Q. Xu, A. Khademhosseini and S. R. Sonkusale, *Microsystems and Nanoengineering*, , DOI:10.1038/micronano.2016.39.

39 X. Li, J. Tian and W. Shen, *ACS Applied Materials \& Interfaces*, 2010, **2**, 1–6.

40 J. Xia, S. Khaliliazar, M. M. Hamedi and S. Sonkusale, *MRS Bulletin*, 2021, **46**, 502–511.

41 K. Khachornsakkul, R. Del-Rio-Ruiz, L. Chheang and S. Sonkusale, *Sensors and Actuators B: Chemical*, 2023, **395**, 134518.

42 P. Singhaphan and F. Unob, *Sensors and Actuators, B: Chemical*, 2021, **327**, 128938.

43 M. Shamsipur, H. R. Rajabi, S. M. Pourmortazavi and M. Roushani, *Spectrochimica Acta - Part A: Molecular and Biomolecular Spectroscopy*, 2014, **117**, 24–33.

44 T. K. Biswas, M. M. Yusoff, M. S. Sarjadi, S. E. Arshad, B. Musta and M. L. Rahman, *Separation Science and Technology (Philadelphia)*, 2021, **56**, 671–680.

45 M. Yasinzai, G. Mustafa, N. Asghar, I. Ullah, M. Zahid, P. A. Lieberzeit, D. Han and U. Latif, *Journal of Sensors*, , DOI:10.1155/2018/8972549.

46 L. D. Mafu, T. A. M. Msagati and B. B. Mamba, *Environmental Science and Pollution Research*, 2013, **20**, 790–802.

47 M. Cejner and R. Dobrowolski, *Annales Universitatis Mariae Curie-Sklodowska, sectio AA – Chemia*, 2016, **70**, 67.

48 K. Huang, Y. Chen, F. Zhou, X. Zhao, J. Liu, S. Mei, Y. Zhou and T. Jing, *Journal of Hazardous Materials*, 2017, **333**, 137–143.

49 H. X. Zhang, Q. Dou, X. H. Jin, D. X. Sun, D. D. Wang and T. R. Yang, *Separation Science and Technology (Philadelphia)*, 2015, **50**, 901–910.

50 Z. Dahaghin, P. A. Kilmartin and H. Z. Mousavi, *Food Chemistry*, 2020, **303**, 125374.

51 Z. Adibmehr and H. Faghihian, *Separation Science and Technology (Philadelphia)*, 2018, **53**, 2388–2400.

52 X. Cai, J. Li, Z. Zhang, F. Yang, R. Dong and L. Chen, *ACS Applied Materials and Interfaces*, 2014, **6**, 305–313.

53 P. Shirazifard, S. Sadjadi, S. J. Ahmadi and F. Faghihi, *Separation Science and Technology (Philadelphia)*, 2016, **51**, 248–254.

54 F. de Liss Meza López, S. Khan, G. Picasso and M. Del Pilar Taboada Sotomayor, *Environmental Nanotechnology, Monitoring and Management*, 2021, **16**, 100497.

55 K. Khachornsakkul and W. Dungchai, *Analytical sciences : the international journal of the Japan Society for Analytical Chemistry*, 2021, **37**, 963–969.

56 L. Chheang, T. Sriwiriyarat, S. P. Thanasupsin and N. Thongkon, *Coloration Technology*, 2023, 1–16.

57 K. Khachornsakkul, R. Del-rio-ruiz, W. Zeng and S. Sonkusale, , DOI:10.1021/acs.analchem.3c01778.

58 B. S. Yew, M. Muhamad, S. B. Mohamed and F. H. Wee, *Sains Malaysiana*, 2019, **48**, 653–659.

59 L. Yan, B. Kasal and L. Huang, *Composites Part B: Engineering*, 2016, **92**, 94–132.

60 A. Nilghaz, D. H. B. Wicaksono, D. Gustiono, F. A. Abdul Majid, E. Supriyanto and M. R. Abdul Kadir, *Lab on a Chip*, 2012, **12**, 209–218.

61 Y. D. Li, W. Y. Li, H. H. Chai, C. Fang, Y. J. Kang, C. M. Li and L. Yu, *Cellulose*, 2018, **25**, 4831–4840.

62 K. Khachornsakkul, W. Dungchai and N. Pamme, *ACS Sensors*, 2022, **7**, 2410–2419.

Zn^{2+} standard added (mg L^{-1})	Total Zn^{2+} found ± SD (mg L^{-1})	%Recovery	%RSD
3.0	3.09 ± 0.47	103.16	5.44
5.0	50.02 ± 0.47	100.48	3.71
7.0	7.11 ± 0.82	101.62	4.80

Table 1. Recovery studies of the detection of Zn^{2+} in human control urine samples (n=3).

Table 2. Result of Zn^{2+} in the supplement sample analysis by our developed method (n=3).

Supplement sample	Total found (mg/tablet)	Specific label (mg/tablet)	T-test	%RSD
A	48.45 ± 0.94	50.0	0.43	4.22

Table 3. Comparison of the proposed method with other methods reported in the literature.

Method	Linear range (mg L^{-1})	LOD (mg L^{-1})	Reference
Colorimetric detection	0.1-1.0	0.02	41
Optical detection	0.02 –3.8	0.005	48
Electrochemical detection	0.2–7.0	0.02	49
Colorimetric detection	0.0 – 0.5	0.02	50
dTADs	1.0-20.0	1.0	This work

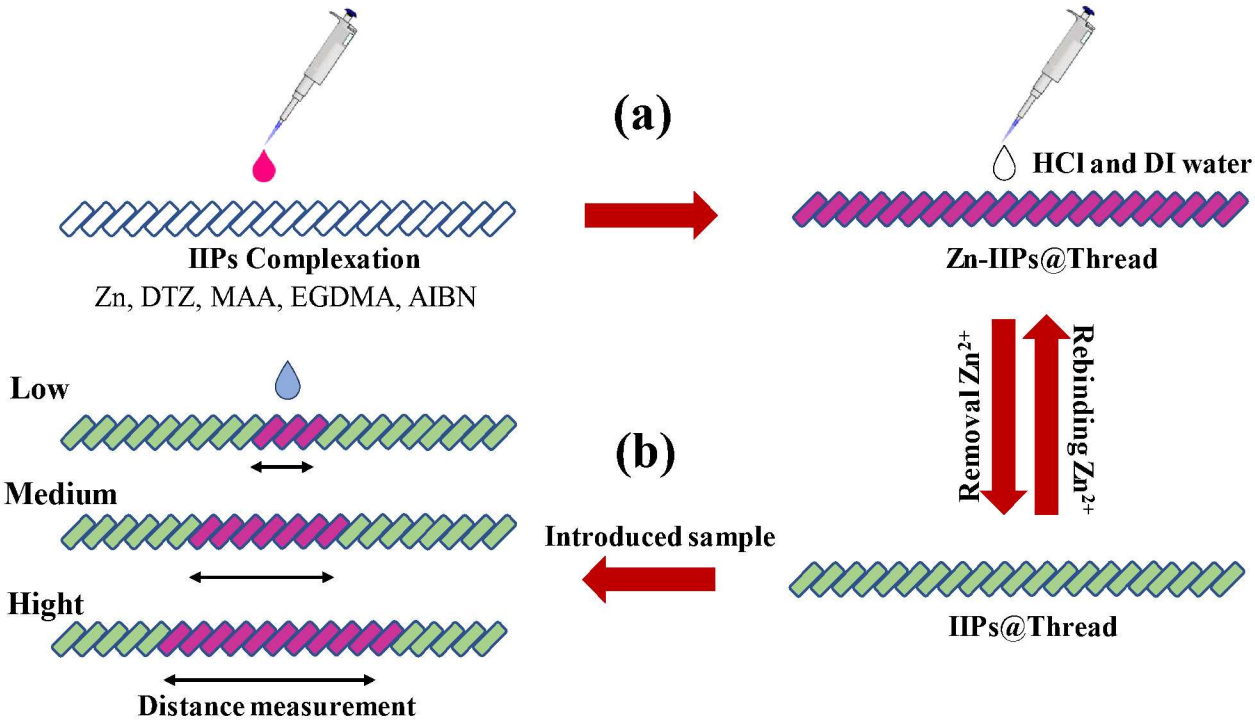

Fig. 1: The scheme of (a) the general fabrication procedure for the IIPs-based dTADs sensor (b) the procedure of Zn^{2+} measurement.

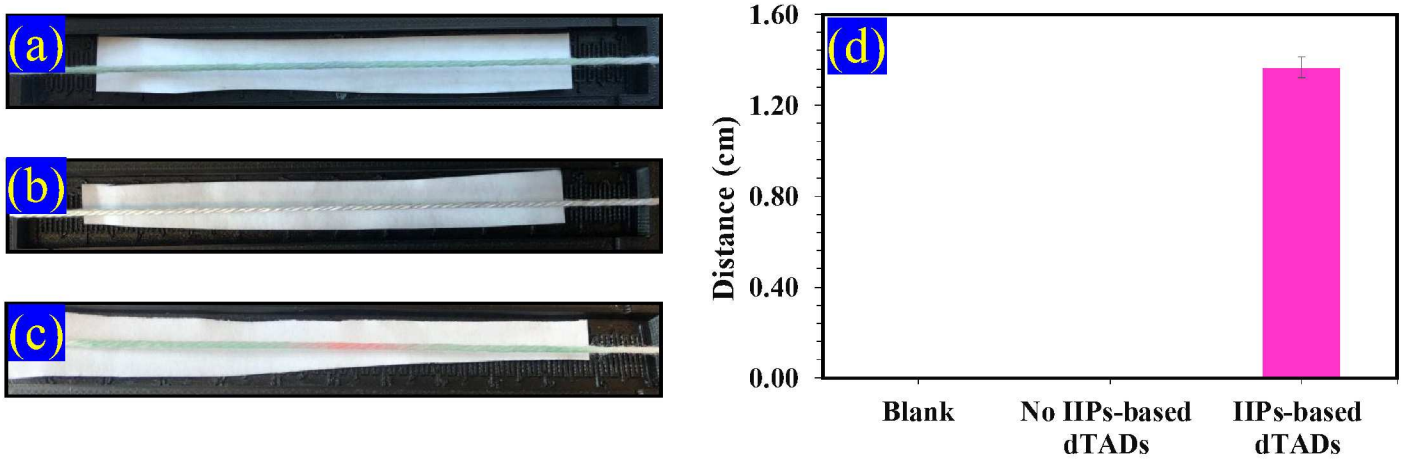

Fig. 2. The image of distance signals of Zn^{2+} detection at 5.0 mg L^{-1} including (a) blank, (b) no IIPs-based dTADs, (c) IIPs-based dTADs, and (d) their distance signals (n=3).

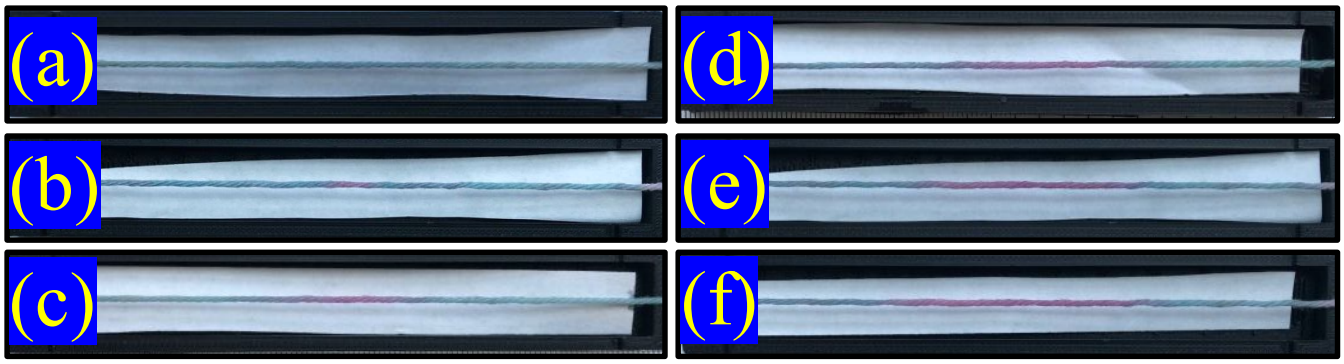
(a)
(d)
(b)
(e)
(c)
(f)

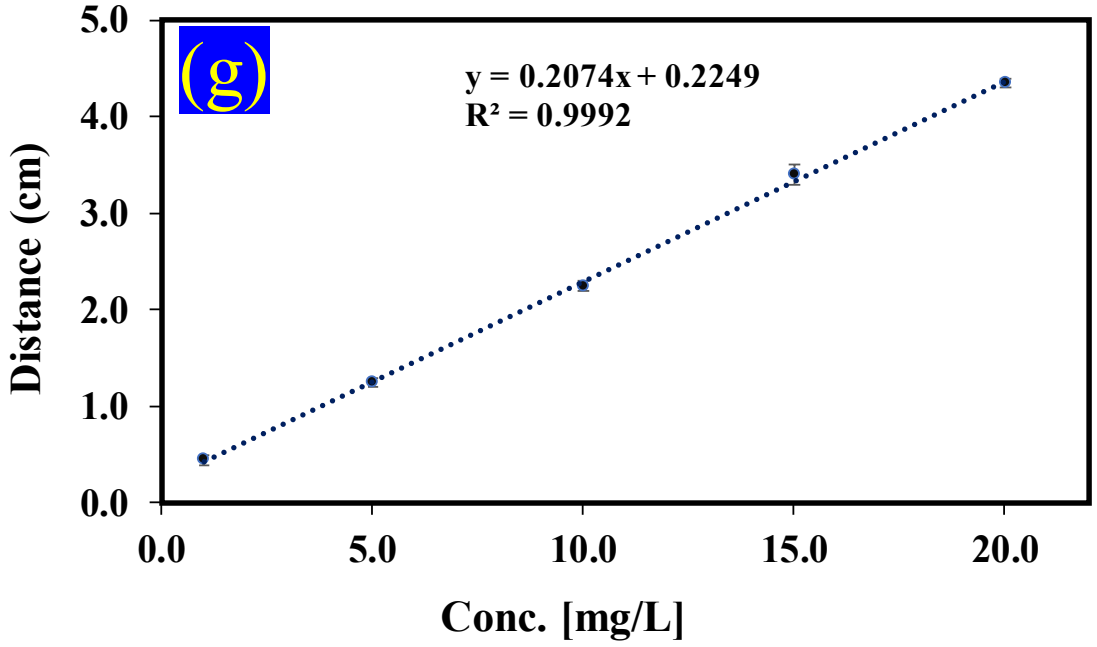
(g)
y = 0.2074x + 0.2249
R² = 0.9992
Distance (cm)
Conc. [mg/L]
0.0
1.0
2.0
3.0
4.0
5.0
0.0
5.0
10.0
15.0
20.0

Fig. 3. The image of the distance signals for Zn^{2+} detection at (a) blank, (b) 1.0, (c) 5.0, (d) 10.0, (e) 15.0, (f) 20.0 mg L^{-1}, and (g) the plotted linear range (n = 3).

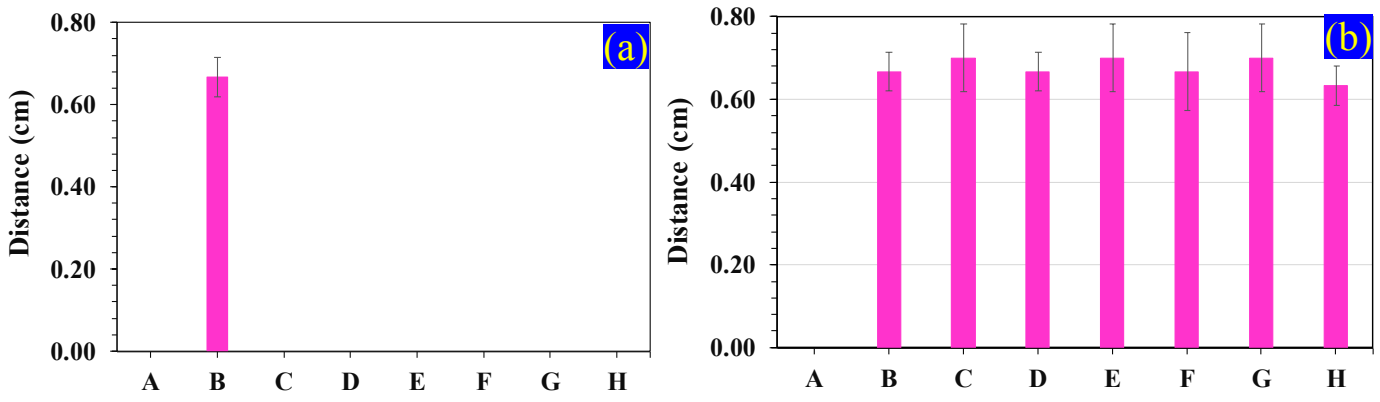

Fig. 4. (a) Selectivity for Zn^{2+} detection; distance signals obtained for (A) a blank solution, (B) Zn^{2+} at 2.0 mg L^{-1}, and solutions of a range of potentially interfering substances including (C) glucose (10.0 mmol L^{-1}), (D) bovine serum albumin (10.0 g L^{-1}), (E) lactic acid (50.0 µmol L^{-1}), (F) uric acid (500.0 µmol L^{-1}), (G) urea (50.0 mmol L^{-1}), and (H) creatinine (1.0 g L^{-1}). (b) Interference for Zn^{2+} detection; distance signals obtained for (A) a blank, (B) Zn^{2+} at 2.0 mg L^{-1}, and (C-H) mixtures of 2.0 mg L^{-1} Zn^{2+} and above concentrations of the potentially interfering substances (n = 3).